

ORIGINAL ARTICLE

Network analysis of gene expression in mice provides new evidence of involvement of the mTOR pathway in antipsychotic-induced extrapyramidal symptoms

S Mas^{1,2,3}, P Gassó^{1,2,3}, D Boloc¹, N Rodríguez¹, F Mármol¹, J Sánchez¹, M Bernardo^{2,3,4,5} and A Lafuente^{1,2,3}

To identify potential candidate genes for future pharmacogenetic studies of antipsychotic (AP)-induced extrapyramidal symptoms (EPS), we used gene expression arrays to analyze changes induced by risperidone in mice strains with different susceptibility to EPS. We proposed a systems biology analytical approach that combined the identification of gene co-expression modules related to AP treatment, the construction of protein–protein interaction networks with genes included in identified modules and finally, gene set enrichment analysis of constructed networks. In response to risperidone, mice strain with susceptibility to develop EPS showed downregulation of genes involved in the mammalian target of rapamycin (mTOR) pathway and biological processes related to this pathway. Moreover, we also showed differences in the phosphorylation pattern of the ribosomal protein S6 (rpS6), which is a major downstream effector of mTOR. The present study provides new evidence of the involvement of the mTOR pathway in AP-induced EPS and offers new and valuable markers for pharmacogenetic studies.

The Pharmacogenomics Journal (2016) **16**, 293–300; doi:10.1038/tpj.2015.48; published online 30 June 2015

INTRODUCTION

Early acute extrapyramidal symptoms (EPS) are serious, debilitating and stigmatizing adverse effects of antipsychotics (AP). Although these side effects usually respond to dose reduction or to additional pharmacological treatment, they are a major cause of poor adherence to AP treatment.¹

Recently, the heritability of EPS was estimated to be ~0.90 using inbred mouse strains exposed to haloperidol.² Despite the existence of this heritability, however, inconsistent results have been obtained in pharmacogenetic studies of EPS. The most promising results involve dopaminergic candidate genes (*DRD3* and *RGS2*)^{3–5} and genes involved in AP pharmacokinetics,^{6,7} although no single factor has been able to predict EPS.^{8,9,10}

Although the exact mechanism underlying EPS is not clear, striatal dopamine D2 receptor (DRD2) blockade is believed to be the principal cause.¹¹ Apart from their receptor-binding profile, little is known about the underlying molecular mechanism by which AP act. One approach that could help to elucidate the molecular signatures of AP treatments involves the study of gene expression.¹² Although gene expression studies have implicated many genes in the pharmacological effect of AP, most results have not been replicated. Therefore, one research avenue involves the search for dysregulated molecular pathways or gene networks inferred from interactome. The advantage of this type of approach is that it has the potential to reconcile poor biomarker reproducibility across studies by identifying common biological pathways or functional modules.¹³

Essential control of motor activity is exerted by dopamine in the striatum.¹⁴ As an evolutionary ancient brain region, the functions

and gene expression profiles of the striatum are comparable between rodents and humans.¹⁵ Thus, despite the limitation of an animal model, the comparison of AP-induced changes in the rodent striatal gene expression profile provides insights into molecular mechanisms of AP actions.¹⁶

In the present study we used whole-genome expression arrays to analyze changes in gene expression induced by treatment with risperidone in two different mice strains (A/J and DBA/2J) with different susceptibility to EPS but a similar metabolic profile (according to Crowley *et al.*²). Weighted co-expression network analysis (WGCNA) was carried out to identify gene co-expression modules related to AP treatment in each strain. In addition, we constructed a protein–protein interaction (PPI) network with genes involved in each co-expression module and performed gene set enrichment analysis to identify molecular pathways and biological processes involved in AP-induced EPS, the aim being to identify potential candidate genes for future pharmacogenetic studies.

MATERIALS AND METHODS

Animals

Male mice (7–8 weeks old) from two inbred strains, A/JOLA-Hsd (A/J) and DBA/2JRCc-Hsd (DBA/2J) (Harlan Laboratories, Sant Feliu de Codines, Spain), were housed eight per cage under a 12-h dark/light cycle with free access to food and water. Mice were allowed to acclimatize to the colony for 1–2 weeks before the initiation of training. All animal-related procedures were in accordance with the European Union guidelines for the care and use of laboratory animals and were approved by the local animal care committee of the University of Barcelona and the Generalitat de Catalunya.

¹Department of Pathological Anatomy, Pharmacology and Microbiology, University of Barcelona, Barcelona, Spain; ²Institut d'Investigacions Biomèdiques August Pi i Sunyer (IDIBAPS), Barcelona, Spain; ³Centro de Investigación Biomédica en Red de Salud Mental (CIBERSAM), Madrid, Spain; ⁴Barcelona Clinic Schizophrenia Unit (BCSU), Psychiatry Service, Hospital Clínic de Barcelona, Barcelona, Spain and ⁵Department Psychiatry and Clinical Psychobiology, University of Barcelona, Barcelona, Spain. Correspondence: Dr A Lafuente, Department of Pathological Anatomy, Pharmacology and Microbiology, University of Barcelona, Casanova 143, Barcelona E-08036, Spain. E-mail: amalialafuente@ub.edu

Received 23 December 2014; revised 10 April 2015; accepted 18 May 2015; published online 30 June 2015

Drug treatment

Mice were injected i.p. (volume 0.25 ml) with risperidone (0.5, 1.0 and 1.5 mg kg⁻¹) or saline once per day for three consecutive days. Injections were performed at 0900–0930 hours. For each strain four groups were created, with six animals per each dose assayed and an appropriate vehicle group (24 animals of each strain were used in the study). Risperidone (Sigma-Aldrich, St Louis, MO, USA) was suspended in water.

Tissue collection and RNA isolation

After three days of treatment, animals were sacrificed by decapitation 2 h after the last injection, and their brains were rapidly removed and placed on ice. The striatum was then dissected out and immediately preserved at –80 °C. Samples were homogenized in Trizol reagent (Life Technologies, Foster City, CA, USA) and RNA was isolated following the manufacturer's protocol, before being further purified using the RNeasy Mini Kit (Qiagen, Valencia, CA, USA). RNA concentrations were determined using a Nanodrop ND-1000 spectrophotometer (Nanodrop, Wilmington, DE, USA). The purity and integrity of RNA was assessed using an Agilent 2100 Bioanalyzer (Agilent Technologies, Palo Alto, CA, USA). A total of 1 µg of purified RNA from each of the samples was submitted to the Kompetenzentrum für Fluoreszenz Bioanalytik Microarray Technology (KFB, BioPark Regensburg GmbH, Regensburg, Germany) for labeling and hybridization to Affymetrix GeneChip Arrays MG 430 PM (Affymetrix, Santa Clara, CA, USA).

Microarray data analysis

Full details of extraction, labeling and hybridization protocols, raw array data (.cel files) and pre-processed data matrix are available at the Gene Expression Omnibus database (<http://www.ncbi.nlm.nih.gov/geo/>; Gene Expression Omnibus accession number GSE67723).

Preprocessing. Microarray data preprocessing analysis was performed using the Babelomics 4.3 suite (<http://www.babelomics.org/>). The data were standardized using robust multichip analysis. Multiple probe mapping to the same gene were merged using the average as the summary of the hybridization values. Formal power analysis was not used to predetermine sample size, however, sample size (four per strain and condition) was determined based on previous estimations to identify greater than twofold change in gene expression levels at $P < 0.01$ using inbred animals.¹⁷ No data points were excluded as outliers. Animal's allocation to treatment was randomized and the experimenter was blinded to the group allocation during motor activity assessment, sample collection and sample processing.

WGCNA procedure. Co-expression modules were identified using the WGCNA R software package (<http://labs.genetics.ucla.edu/horvath/CoexpressionNetwork/Rpackages/WGCNA/>).¹⁸ The co-expression analysis starts by constructing a matrix of pairwise correlations between all pairs of genes across all selected samples. Next, the matrix is raised to a soft-thresholding power ($\beta=8$ in this study) to obtain an adjacency matrix. In order to identify modules of co-expressed genes, we constructed the topological overlap-based dissimilarity,¹⁸ which was then used as input to average linkage hierarchical clustering. This step results in a clustering tree (dendrogram) whose branches are identified for cutting depending on their shape using the dynamic tree-cutting algorithm.¹⁸ The above steps were performed using the automatic network construction and module detection function (*blockwiseModules* in WGCNA), with the following major parameters: *minModuleSize* of 30; *reassignThreshold* of 0; and *mergeCutHeight* of 0.25. The modules were then tested for their associations with the trait by correlating module eigengenes with trait measurements.

PPI network construction and evaluation. Genes included in each gene co-expression module that were significantly associated with AP treatment in each strain were used to create PPI networks. Gene mice were converted to human orthologs in order to use the most curated human interactome. The SNOW program (<http://www.babelomics.org/>), implemented in the Babelomics 4.3 suite, was used for the analysis.¹⁹ The minimum connected network (MCN), defined as the shortest network that connects all the interacting nodes within a gene list, was obtained as described previously.²⁰ Briefly, we used the curated interactome (validated by at least two independent methods) and allowed the inclusion of extra nodes that connect two or more nodes in the list. Network enrichment analysis was performed to test whether the parameters that described a network

were beyond their random expectations or not. The parameters analyzed were connection degree, clustering coefficient and betweenness centrality.^{19,20}

Gene set enrichment analysis and visualization. The MCN constructed with SNOW for each gene co-expression module associated with AP treatment was uploaded into Cytoscape 3.0.2 (<http://www.cytoscape.org>). We then used ClueGO v2.1 (<http://apps.cytoscape.org/apps/cluego>), a Cytoscape plug-in,²¹ to perform a gene set enrichment analysis as described previously.²⁰ Briefly, we selected the unstructured terms of biological processes from Gene Ontology (GO) (<http://geneontology.org/>) and Reactome pathways (<http://www.reactome.org/>). Only terms with an adjusted P -value < 0.05 and experimental evidence were selected for analysis. Genes involved in each MCN were mapped to their enriched term based on the hypergeometric test (two sided), with the P -value being corrected by the Benjamini–Hochberg method. ClueGO created a functional module network in which the different GO terms or Reactome pathways were clustered according to the association strength between terms calculated using chance-corrected kappa statistics.²¹

Motor activity assessment

The effect of risperidone on motor activity was measured by three different methods.

Rotarod. Motor coordination and balance were evaluated on the rotarod apparatus as described elsewhere.²² For rotarod learning assessment, mice were trained at a fixed speed of 20 r.p.m. and subsequently tested with two trials per day spaced 1 h apart over two consecutive days. For the accelerating task, the rotarod was accelerated from 5 to 40 r.p.m. over 5 min. Rotarod testing was performed twice a day with a 1-h interval. The latency to fall was recorded for each of the two trials and averaged.

Catalepsy test. Catalepsy was measured by using a standard bar test, in which the mouse was maintained in an imposed position with both front limbs extended and resting on a 5-cm high bar (0.4 cm in diameter). The end point of catalepsy was considered to be the point either at which one of the front paws was removed from the bar or the mouse moved its head in an exploratory manner. The cutoff time was 720 s.

Open-field test. Spontaneous locomotor activity was measured using the open-field test.²³ Briefly, the apparatus consisted of a white circular arena measuring 40 cm in diameter and 40 cm in height. Dim light intensity was 40 lux throughout the arena. Animals were placed on the arena center and allowed to explore freely for 30 min. Spontaneous locomotor activity was measured. Animals were tracked and recorded with SMART junior software (Panlab, Barcelona, Spain). We extracted as phenotype the total distance traveled (cm).

Western blotting

Striatum samples were homogenized in Trizol reagent (Life Technologies) and proteins were isolated following the manufacturer's protocol. Aliquots of the homogenate were used for protein determination using a Lowry assay. Equal amounts of protein for each sample were loaded onto 10% polyacrylamide gels. Proteins were separated by SDS–polyacrylamide gel electrophoresis and transferred using iBlot Transfer Stacks (Life Technologies). The membranes were immunoblotted using antibodies against phospho-Ser235/236-rpS6 and phospho-Ser244/247-rpS6 (Cell Signaling Technology, Beverly, MA, USA). Antibodies against rpS6 (Cell Signaling Technology), which are not phosphorylation state specific were used to estimate the total amount of protein. Chemoluminescent images were acquired with a LAS-3000 Imager (Fujifilm, Valhalla, NY, USA). The levels of each phosphoprotein were normalized for the amount of the corresponding total protein detected in the sample.

Statistical analysis

Statistical analyses were performed in GraphPad Prism version 5.00 for Windows (GraphPad Software, San Diego, CA, USA) or SPSS version 17 (SPSS, Chicago, IL, USA). Normal distributions of the data were confirmed using Shapiro–Wilk test, and equality of the variance between groups was assessed by means of Levene's test. For comparing two groups, a two-tailed Student's t -test was used. Significance was set at $P < 0.05$.

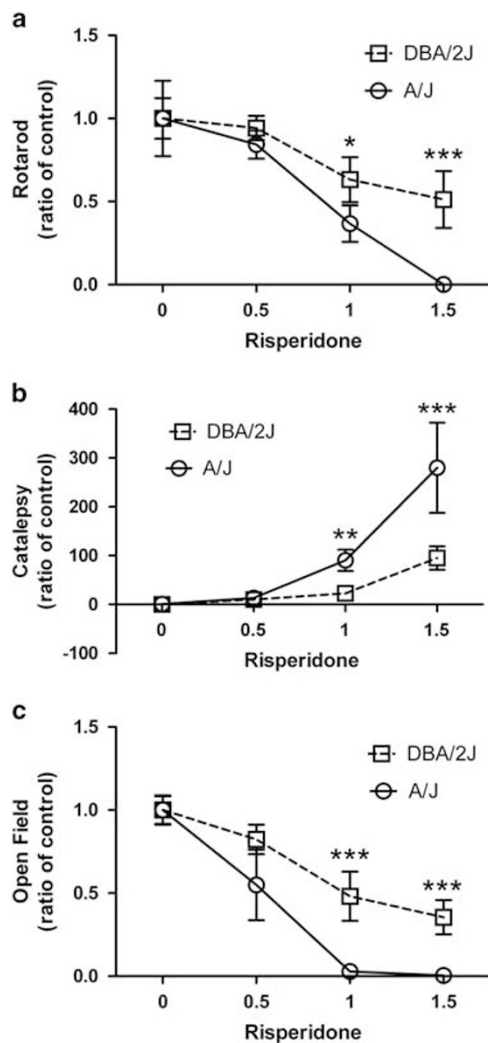


Figure 1. The effect of risperidone on motor activity in two different mice strains (A/J and DBA/2J) with different susceptibility to extrapyramidal symptoms. Motor activity was measured by three different methods: (a) rotarod; (b) catalepsy test; and (c) open field. The x axis showed risperidone dosage (mg kg⁻¹) and the y axis gives the phenotypic value of each method expressed as ratio of control treatment. All graphs are average \pm s.d. of six replicates and analyzed by Student's *t*-test for statistical differences. **P* < 0.05, ***P* < 0.01, ****P* > 0.001.

RESULTS

Motor assessment

First, we evaluated the motor effects of different risperidone dosages on A/J and DBA/2J strains. It can be seen in Figure 1 that with doses of 1 mg kg⁻¹ or higher, A/J mice suffered greater motor impairment than did DBA/2J animals: the time to fall from the rotarod was shorter ($t_8 = -3.03$, $P = 0.02$; Figure 1a), the time to remove the front paws in the catalepsy test was longer ($t_8 = 5.18$, $P = 0.002$; Figure 1b) and the distance traveled in the open-field test was shorter ($t_8 = -6.06$, $P = 0.0009$; Figure 1c). These results are in agreement with those obtained by Crowley *et al.*,² and we therefore consider A/J as the strain 'susceptible to EPS' and DBA/2J as the strain 'resistant to EPS'. As significant differences in motor activity could be observed at risperidone 1 mg kg⁻¹, we used this dosage for the gene expression analysis. For each strain a saline group and a treatment group of four replicates each were used (8 microarrays for each strain, 16 microarrays in total). For

each group the four samples with highest RNA purity were selected.

Gene co-expression network construction and relation to AP treatment

We applied WGCNA to genome-wide data to identify 'modules' of co-expressed genes. Figure 2 shows the cluster dendrogram obtained for each strain, A/J (Figure 2a) and DBA/2J (Figure 2b). We identified 97 modules in the A/J strain and 58 modules in the DBA/2J strain. One module of the A/J strain, the Salmon module (382 genes), showed a significant negative correlation with treatment (false discovery rate (FDR)-corrected P -value < 0.001). In the DBA/2J data set, two modules, Yellow (990 genes) and Sky Blue (237 genes), presented a significant positive correlation with treatment (FDR-corrected P -value < 0.001).

PPI network construction

Genes included in each module significantly associated with risperidone treatment were used to construct PPI networks. The MCN constructed with genes of the Salmon module (Figure 3a) in the A/J data set comprised 774 gene products and included 166 of the 382 expressed genes in the module (43.45%). External nodes represented 78.55% of all nodes in the MCN. The node of the obtained PPI network showed more connections (connectivity degree P -value = 8×10^{-3}), greater connectivity (clustering coefficient P -value = 7×10^{-3}) and more hub nodes (betweenness centrality P -value = 7×10^{-3}) in comparison with random expectations.

The MCN constructed with genes of the Yellow module (Figure 3b) in the DBA/2J data set comprised 175 gene products and included 129 of the 990 expressed genes (13.03%) in the module. External nodes represented 26.28% of all nodes in the MCN. The node of the obtained PPI network showed more connections (connectivity degree P -value = 5×10^{-3}), greater connectivity (clustering coefficient P -value = 3×10^{-2}) and more hub nodes (betweenness centrality P -value = 2×10^{-2}) in comparison with random expectations. The Sky Blue module (Figure 3c) from the same data set comprised 67 gene products and included 51 of the 237 expressed genes (21.51%) in the module. External nodes represented 23.88% of all nodes in the MCN. The node showed more connections (connectivity degree P -value = 3×10^{-2}), greater connectivity (clustering coefficient P -value = 3×10^{-2}) and more hub nodes (betweenness centrality P -value = 1×10^{-2}) in comparison with random expectations.

Gene set enrichment analysis

MCN constructed with the Salmon module genes were enriched by 19 clusters that comprised 95 terms (Supplementary Table S1). Each cluster represented different GO terms or Reactome pathways with high association strength calculated using chance-corrected kappa statistics. In order to present a more comprehensible analysis, Table 1 shows the clusters of GO terms of the hub genes, those with greater connectivity and betweenness, in the Salmon module. Sixteen GO terms were clustered into three groups namely lipid and glucose metabolism, autophagy and response to nutrient levels. The gene set enrichment analysis with Reactome pathways identified four significant terms in the Salmon module: mammalian target of rapamycin (mTOR) signaling (term P -value FDR corrected 9.5×10^{-10}); signaling by NOTCH1 (term P -value FDR corrected 4×10^{-3}); constitutive PI3/AKT signaling in cancer (term P -value FDR corrected 1.4×10^{-4}); and PI3K cascade (term P -value FDR corrected 2.5×10^{-9}).

Table 1 shows the 11 clusters of GO terms identified in the MCN constructed with genes involved in the Yellow module of the DBA/2J data set. Among these clusters, the most significant and those including most GO terms were related to synaptic transmission

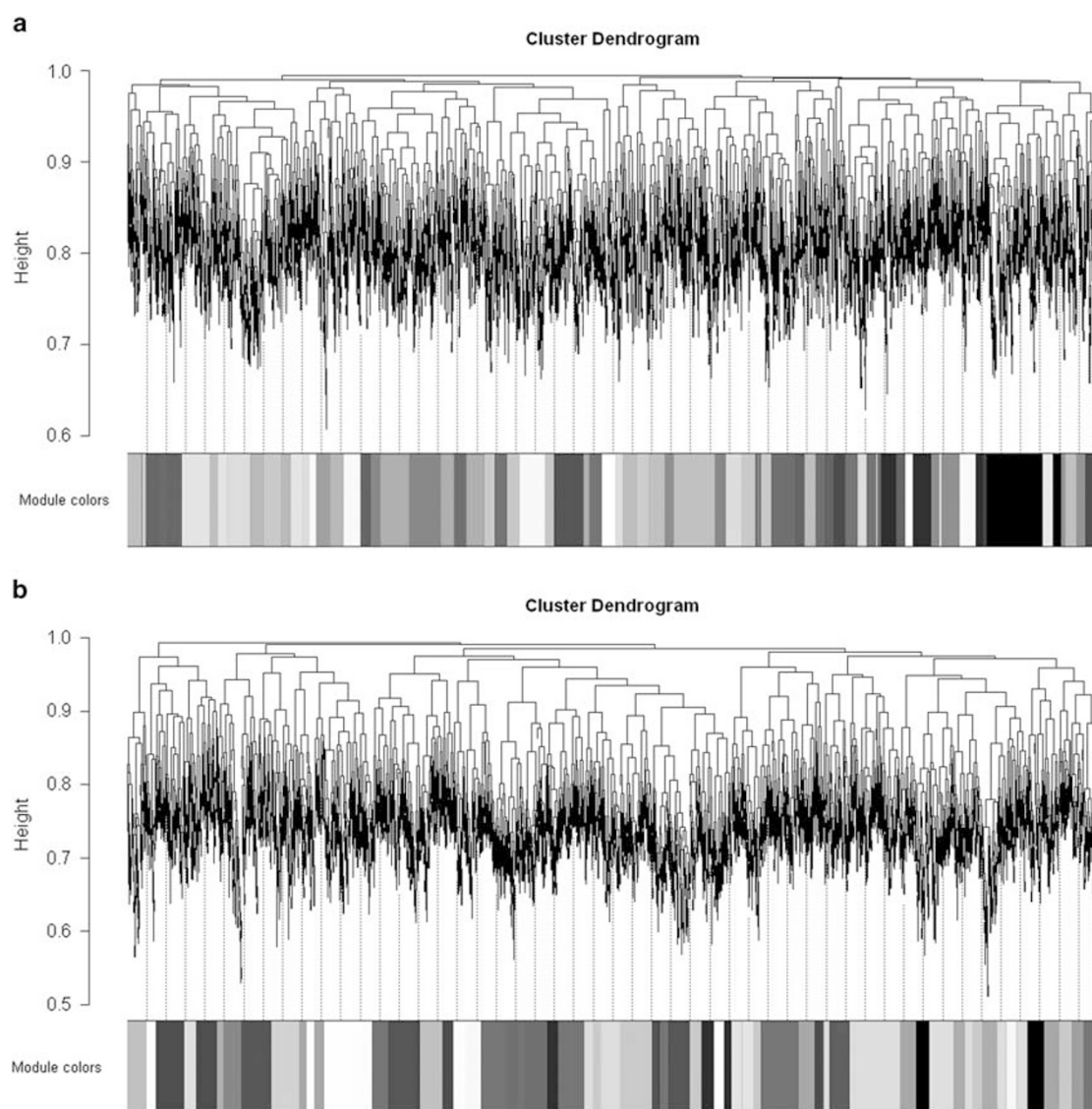


Figure 2. Gene co-expression networks obtained for each strain, A/J (a) and DBA/2J (b). Branches in the hierarchical clustering dendrograms correspond to modules. Modules of co-expressed genes were assigned colors corresponding to the branches. A full color version of this figure is available at *The Pharmacogenomics Journal* online.

(cluster 3) and neuron differentiation (cluster 4). Accordingly, the significantly enriched Reactome pathways were related to these processes: γ -aminobutyric acid synthesis, release, reuptake and degradation (term P -value FDR corrected 9.6×10^{-4}); activation of N -methyl-D-aspartate receptor upon glutamate binding and postsynaptic events (term P -value FDR corrected 1.6×10^{-6}); and regulation of actin dynamics for phagocytic cup formation (term P -value FDR corrected 2.3×10^{-7}).

The Sky Blue module was enriched with 12 GO terms clustered into four groups (Table 1), with the largest cluster being related to synaptic vesicle transport. Two Reactome pathways were significantly enriched in this MCN: clathrin-derived vesicle budding (term P -value FDR corrected 1×10^{-2}) and translocation of GLUT4 to the plasma membrane (term P -value FDR corrected 9.5×10^{-3}).

Western blot

In order to confirm that the most significantly enriched pathway in our samples, namely the mTOR pathway, was really differentially affected in mice strains with different susceptibility to EPS, we

studied the phosphorylation pattern of the ribosomal protein S6 (rpS6), which is phosphorylated by a major downstream effector of mTOR. Two phosphorylation sites were studied: Ser235/236 and Ser244/247. In the A/J mice, with greater susceptibility to develop EPS, administration of risperidone at 1 mg kg^{-1} produced a twofold increase in the levels of phosphorylation at Ser235/236 ($t_6 = 2.71$, $P = 0.03$) and a more than 80% decrease in phosphorylation at Ser244/247 ($t_6 = 4.58$, $P = 0.003$; Figure 4a). The opposite effect was observed in DBA/2J mice (resistant strain to EPS) as in this case administration of risperidone at 1 mg kg^{-1} produced a 60% decrease in phosphorylation at Ser235/236 ($t_6 = 7.16$, $P = 0.0008$) and a more than threefold increase in Ser244/247 phosphorylation ($t_6 = 2.27$, $P = 0.05$; Figure 4b).

DISCUSSION

Our study revealed that in response to risperidone, mice strain with susceptibility to develop motor side effects (A/J) in the striatum showed downregulation of genes involved in the mTOR pathway and biological processes related to these genes such as

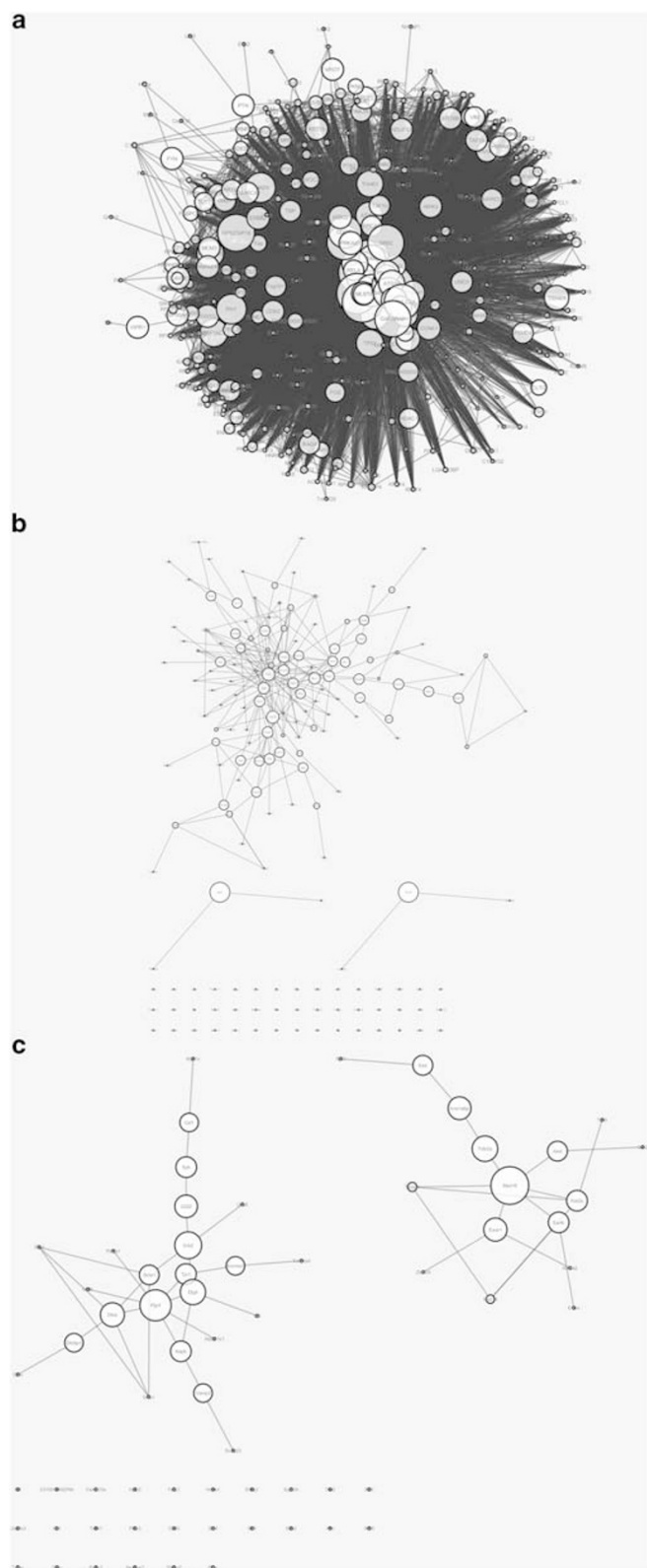


Figure 3. Protein–protein interaction network constructed using modules of co-expressed genes significantly associated with 1 mg kg^{-1} risperidone treatment for each strain: Salmon module (a) in A/J strain; and Yellow module (b) and Sky Blue module (c) in DBA/2J strain.

autophagy, lipid and glucose metabolism, and response to nutrient levels. Moreover, signaling cascades related to mTOR activity, such as NOTCH1²⁴ and PI3K/AKT,²⁵ were also involved in the response. By contrast, in the striatum of mice resistance to EPS (DBA/2J), the response to risperidone involved upregulation of processes involved in synaptic transmission, synaptic vesicle formation and neuron differentiation, with pathways related to γ -aminobutyric acid, glutamate and actin cytoskeleton.

The mTOR pathway was identified in the gene set enrichment analysis performed with the MCN constructed with genes co-expressed in the Salmon module. This MCN showed a higher percentage of external nodes (78.55%) than the MCNs constructed with genes co-expressed in the Yellow and the Sky Blue nodes (26.28% and 23.88% respectively). We performed separate gene set enrichment analysis of these genes from the Salmon module and the external genes included in the MCN in order to see if the mTOR enrichment is exclusively related to external nodes. None of the analysis identified the mTOR pathway. This is in agreement with the fact that differential gene expression data reveals only that part of the functional mode, which shows different behavior among the conditions studied, providing an incomplete description of the functionalities operating in the compared conditions. The approach followed here that allows the introduction of extra nodes not differentially expressed reveals a picture much closer to the real functional modules operating in the conditions compared.¹³

Recent studies by our group have also related the mTOR pathway to the appearance of EPS.^{20,26} In one study we performed a network analysis of differential gene expression induced by AP treatment in peripheral blood of AP-naïve patients with first-episode psychosis.²⁰ This analysis revealed that constructed networks with downregulated genes in patients presenting EPS were enriched for mTOR pathway and different biological processes directly related to this pathway (insulin receptor signaling, lipid modification and regulation of autophagy).²⁰ In another study we used four SNPs in four genes involved in the mTOR pathway to develop a predictor of EPS.²⁶ This pharmacogenetic predictor, including the SNPs rs1130214 (*AKT1*), rs456998 (*FCHSD1*), rs7211818 (*Raptor*) and rs1053639 (*DDIT4*) correctly predicted 85% of EPS appearance in three different cohorts.²⁶

We do not test changes in gene expression with other antipsychotics so we are unable to ensure that these alterations in the mTOR pathway could be extended to other drugs than risperidone. However, recently, different groups of researchers have demonstrated that the mTOR pathway may be modulated by several AP such as chlorpromazine,²⁷ olanzapine,²⁸ haloperidol²⁹ and risperidone.¹⁶

The present study also showed differences between the two mice strains in the phosphorylation pattern of the rpS6, which is phosphorylated by the p70 rpS6 kinase (S6K) 1, a major downstream effector of mTOR. rpS6 is phosphorylated at two sites: Ser244/247, by mTOR-S6K1,³⁰ and Ser235/236 via p90 ribosomal S6 kinases, which are activated, respectively, by extracellular signal-regulated kinases³¹ and protein kinase A (PKA).³² In our study, mice with the strain conferring susceptibility to EPS showed downregulation of networks involving the AKT/mTOR pathway, as well as diminished phosphorylation of rpS6 Ser244/247 and increased phosphorylation of Ser235/236. By contrast, mice with the strain conferring resistance to EPS showed increased phosphorylation of rpS6 Ser 244/247.

Several studies, using haloperidol, have identified rpS6 phosphorylation as a downstream mechanism of AP signaling in DRD2 expressing neurons of the striatum.^{29,33,34} However, whether this regulation is dependent on mTOR signaling is still controversial. Valjent *et al.*³³ observed *in vivo* an increase in Ser235/236 phosphorylation in response to haloperidol 0.5 mg kg^{-1} after 15 min of treatment. This effect was independent of mTOR and related to PKA.³³ By contrast, after 60 min with the same treatment, Bonito-

Table 1. Gene set enrichment analysis of biological processes from GO obtained from constructed PPI networks of each significant module identified in the WGCNA

Clusters	Function	GO biological process terms	Genes
<i>Salmon module network (A/J strain)</i>			
Cluster 0	Lipid and glucose metabolism	GO:0031331; GO:0006110; GO:0006853; GO:0008286; GO:0010906; GO:0010907; GO:0019217; GO:0032006; GO:0046890	BECN1, HIF1A, FOXO3, MLST8, PDPK1, PIK3C2A, PRKAA1, PRKAA2, PRKAB2, PRKAG1, PRKAG2, STK11
Cluster 1	Autophagy	GO:0006914; GO:0007033; GO:0010506; GO:0016236	ATG10, ATG101, ATG16L1, ATG4C, ATG5, BECN1, CLN3, GABARAP, GABARAPL2, GABARAPL3, MAP1LC3A, MAP1LC3B, MAP1LC3C, PRKAA1, PRKAA2, RAB24, SQSTM1, STK11, ULK1, ULK2, UVRAG, WIPI2
Cluster 2	Response to nutrient levels	GO:0031667; GO:0031669; GO:0032107	ATG101, ATG16L1, ATG4C, ATG5, BECN1, CLN3, DDIT3, MAP1LC3A, PRKAA1, PRKAA2, SNW1, SQSTM1, ULK1, ULK2, WIPI2
<i>Yellow module network (DBA/2J strain)</i>			
Cluster 0	MAP kinase activity	GO:0018107; GO:0043405; GO:0000187; GO:0021537; GO:0021772; GO:0021872; GO:0043406; GO:0043507	EGF, DLX1, FZD8, GRIN1, LRRK2, LYN, MAP2K1, NUMB, PAK1, PDPK1, RAC1, SPAG9, SPRY2, WNT5A
Cluster 1	Metal ion transport	GO:0006816; GO:0010522; GO:0010959; GO:0051238; GO:0051924; GO:0051928; GO:0060402; GO:2000021	ADRB1, ARRB2, CASK, DBI, DLG1, EGF, GNB5, GRIN1, GRIN2B, LYN, MGEA5, PLCG2, PRKCE, RYR1, SLC30A4, YWHAH
Cluster 2	Response to hypoxia	GO:0001666; GO:0071456	ARNT2, KCNMA1, P4HB, PAK1, PDPK1, PRKCE, RYR1, SLC9A1
Cluster 3	Synaptic transmission	GO:0001964; GO:0001967; GO:0007215; GO:0007268; GO:0007270; GO:0007611; GO:0007612; GO:0007617; GO:0008306; GO:0008542; GO:0035235; GO:0035249; GO:0042391; GO:0044708; GO:0048167; GO:0048169; GO:0050804; GO:0050806; GO:0050885; GO:0050905; GO:0051899; GO:0060078; GO:0060291; GO:0006887; GO:0017156; GO:0017157; GO:0045921; GO:0060627; GO:0007269; GO:0046928; GO:0048489; GO:0051650	Adrb1, App, Arrb2, Braf, Btg2, Dbi, Dlg1, Dlg4, Gria2, Gria3, Grid2, Grin1, Grin2b, Gm3, Kcnma1, Lin7a, Lrrk2, Lrn, Map2k1, Mapk3, Man2b1, Mgea5, Mpdz, Myh14, Nab, Nrxn3, Pak1, Pdpk1, Pou5f1, Park2, Prkce, Pou5f1, Ptn, Ptprf, Snap25, Sncaip, Stx1a, Stxbp5, Syt1, Sytl1, Wnt5a, Xbp1, Ywhah
Cluster 4	Neuron differentiation	GO:0016358; GO:0048813; GO:0048814; GO:0060997; GO:0035640; GO:0007416; GO:0051705; GO:0007528; GO:0050803; GO:0051963; GO:0010721; GO:0010769; GO:0010975; GO:0031344; GO:0031345; GO:0045664; GO:0048812; GO:0050775	App, Braf, Caprin1, Dcc, Dlg4, Dlx1, Fzd8, Grid2, Grin1, Grin2b, Hoxa2, Klf5, Lgals1, Lrrk2, Lrn, Map2k1, Meis1, Ngef, Nrxn3, Ntm, Numb, Pak1, Ptprf, Rac1, Spag9, Stmn1, Stxbp5, Ttc3, Vil1, Wnt5a, Ywhah
Cluster 5	Developmental maturation	GO:0050808; GO:0021700; GO:0002064; GO:0002066; GO:0002070; GO:0048469	App, Dlg4, Grin1, Hoxb13, Kcnma1, Klf5, Lrrk2, Nrxn3, Pak1, Pgr, Pdpk1, Rac1, Ryr1, Tfcp2l1, Wnt5a, Xbp1
Cluster 6	Protein polymerization	GO:0032272; GO:0051258; GO:0022411; GO:0032984	Apaf1, Capg, Dlg1, Klc1, Lrn, Mgea5, Prkce, Rac1, Stmn1, Tubb2a, Vil1
Cluster 7	Protein acetylation	GO:0006473; GO:0016573; GO:0043966	Kat2a, Kat5, Mapk3, Mgea5, Nupr1, Supt3, Tada2a
Cluster 8	Innate immune response	GO:0002221; GO:0002224; GO:0045088	Arrb2, Lsm14a, Ly96, Lrn, Pdpk1, Prkce, Rps19, Wnt5a
Cluster 9	Regulation of binding	GO:0043388; GO:0043393; GO:0051098; GO:0051101	App, Arrb2, Carm1, Dot1l, Egf, Mapk3, Parp1, Pitx2, Runx1t1, Spag9
Cluster 10	Actin filament organization	GO:0007015; GO:0032970; GO:0051017; GO:0051492; GO:0051495	Adrb1, Braf, Capg, Crk, Dlg1, Pak1, Park2, Prkce, Rac1, Synpo, Vil1
<i>Sky Blue module network (DBA/2J strain)</i>			
Cluster 0	Synaptic vesicle transport	GO:0007269; GO:0048489; GO:0051640; GO:0060627	Braf, Dlg4, Dmd, Dtnbp1, Napb, Snap23, Syk, Vamp2
Cluster 1	Morphogenesis	GO:0048754; GO:0061138	Csf1, Grb2, Plxna1, Six4, Sox2, Wt1
Cluster 2	Differentiation	GO:0032944; GO:0045670; GO:1902105	Apc, Cd40, Csf1, Esrra, Foxj1, Syk, Tcf3, Tob2
Cluster 3	Acetylation	GO:0006475; GO:0018394; GO:0043966	Kat2a, Tada2a, Taf6l, Tcf3

Abbreviations: GO, Gene Ontology; PPI, protein–protein interaction; WGCNA, weighted co-expression network analysis. The table shows the GO terms identified, their cluster distribution according to ClueGO and the genes involved in each group cluster.

Oliva *et al.*²⁹ observed an increase in Ser240/244 phosphorylation. This increase seems to be related to the inhibitory effect of PKA/dopamine–cAMP-regulated phosphoprotein with molecular weight 32 (DARPP-32) on protein phosphatase 1, which suppresses dephosphorylation of Ser240/244, rather than to a stimulatory effect on mTOR signaling.²⁹ The explanation is that basal activity of mTOR is sufficient to enhance Ser240/244 phosphorylation in the presence of haloperidol.²⁹ By contrast, in a study of primary striatal neuron cultures exposed to a 20-min treatment with 20 nM haloperidol over 7 days, Bowling *et al.*³⁴ observed increased activation of Ser240/244 phosphorylation in conjunction with mTOR activation that was mediated by AKT. This activation led to an enhancement of protein synthesis in cultured neurons and an increase in neuron complexity *in vivo*.³⁴

The differences in rpS6 responsiveness among studies could be due to differences in doses and modes of administration of haloperidol. It is known that, depending on its duration, activation of D2-type DA receptors differentially regulates Akt-dependent pathways. In various models of cells in culture, stimulation of D2R rapidly activates Akt signaling.³⁵ By contrast, prolonged

stimulation of D2-type receptors (over 30–60 min) decreases Akt phosphorylation.³⁶

In this context, it should be noted that several receptors affected by AP, such as D2 and D3, 5-HT_{2A}, and muscarinic receptors, are seven-transmembrane domain proteins coupled to G proteins. The various functions of G-protein-coupled receptors have been associated with the regulation of cAMP and PKA via G-protein-dependent signaling. There is growing evidence that the different ways in which antipsychotics modulate the cAMP and PKA pathway may contribute to their differing clinical and/or side-effect profiles.³⁷ Current data also suggest that the different effects of typical and atypical antipsychotics on cAMP and PKA are complex and region dependent, possibly due to their affinities for different G-protein-coupled receptors that stimulate adenylyl cyclase signaling.³⁸

The main limitation of the present study is that we do not control for risperidone plasma levels. We selected two different mice strains with different susceptibility to develop extrapyramidal symptoms, but with similar metabolic profile, as suggested by Crowley *et al.*² However, the study of Crowley *et al.*² was done

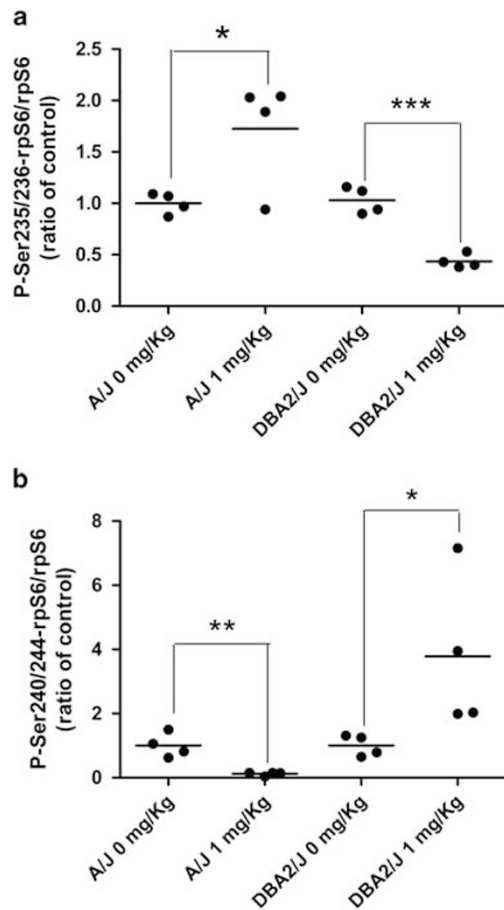


Figure 4. Western blot analysis of the phosphorylation pattern of the ribosomal protein S6 (rpS6). Two phosphorylation sites, Ser235/236 (a) and Ser244/247 (b), were studied in two different mice strains (A/J and DBA2/J). The x axis showed treatment: control (0 mg kg⁻¹) or risperidone 1 mg kg⁻¹. The y axis gives the quantification of phosphorylated rps6 corrected by total rps6 and expressed as ratio of control treatment. Data were analyzed by Student's *t*-test for statistical differences. **P* < 0.05, ***P* < 0.01, ****P* > 0.001.

with haloperidol instead of risperidone. Although both drugs are metabolized by the CYP2D6, other cytochromes are involved in the metabolism of each drug. However, we were unable to obtain enough blood volume of each animal to measure plasmatic risperidone levels with the methodology available in our facilities.

The present study provides new evidence of the involvement of the mTOR pathway in AP-induced EPS. The integration of pharmacogenomic data from animal models (as in the case of the results presented here) with data from microarrays of differentially expressed genes from *in vitro* models³⁹ and peripheral blood in humans²⁰ is the ultimate goal of this research, and it represents an example of the convergent functional genomic approach.¹² These results highlight the importance of integrating pharmacogenomic data from gene expression experiments with systems biology analysis to increase our understanding of the molecular mechanisms of action of antipsychotic drugs. In agreement with recent suggestions by the US National Institute of Mental Health, we focus on understanding the core mechanisms involved in drug response in order to identify networks and pathways that could be affected, rather than on the analysis of independent genes with small effects on drug response.⁴⁰ The ability to study combinations of variants in genes involved in these identified networks and pathways is more likely, than is the study of individual genes, to yield

insight into AP response mechanisms and, therefore, to suggest drug targets.⁴¹

CONFLICT OF INTEREST

The authors declare no conflict of interest.

ACKNOWLEDGMENTS

This study was supported by the Spanish Ministry of Health, Instituto de Salud Carlos III (FIS, Fondo de Investigación Sanitaria PI10/02430) and the Catalan Innovation, Universities and Enterprise Authority (Grants DURSI 2014SGR436 and 2014SGR441). We thank the Language Advisory Service of the University of Barcelona, Spain for manuscript revision. The authors also thank Ana Meseguer for sample collection assistance.

REFERENCES

- Divac N, Prostran M, Jakovcevski I, Cerovac N. Second-generation antipsychotics and extrapyramidal adverse effects. *Biomed Res Int* 2014; **2014**: 656370.
- Crowley JJ, Kim Y, Szatkiewicz JP, Pratt AL, Quackenbush CR, Adkins DE *et al*. Genome-wide association mapping of loci for antipsychotic-induced extrapyramidal symptoms in mice. *Mamm Genome* 2012; **23**: 322–335.
- Greenbaum L, Strous RD, Kanyas K, Merbl Y, Horowitz A, Karni O *et al*. Association of the RGS2 gene with extrapyramidal symptoms induced by treatment with antipsychotic medication. *Pharmacogenet Genomics* 2007; **17**: 519–528.
- Gassó P, Mas S, Bernardo M, Alvarez S, Parellada E, Lafuente A. A common variant in DRD3 gene is associated with risperidone-induced extrapyramidal symptoms. *Pharmacogenomics J* 2009; **9**: 404–410.
- Gassó P, Mas S, Oliveira C, Bioque M, Parellada E, Bernardo M *et al*. Searching for functional SNPs or rare variants in exonic regions of DRD3 in risperidone-treated patients. *Eur Neuropsychopharmacol* 2011; **21**: 294–299.
- Crescenti A, Mas S, Gassó P, Parellada E, Bernardo M, Lafuente A. Cyp2d6*3, *4, *5 and *6 polymorphisms and antipsychotic-induced extrapyramidal side-effects in patients receiving antipsychotic therapy. *Clin Exp Pharmacol Physiol* 2008; **35**: 807–811.
- Mas S, Gassó P, Alvarez S, Parellada E, Bernardo M, Lafuente A. Intuitive pharmacogenetics: spontaneous risperidone dosage is related to CYP2D6, CYP3A5 and ABCB1 genotypes. *Pharmacogenomics J* 2012; **12**: 255–259.
- Lencz T, Malhotra AK. Pharmacogenetics of antipsychotic-induced side effects. *Dialogues Clin Neurosci* 2009; **11**: 405–415.
- Llerena A, Berecz R, Peñas-Lledó E, Süveges A, Fariñas H. Pharmacogenetics of clinical response to risperidone. *Pharmacogenomics* 2013; **14**: 177–194.
- Almoguera B, Riveiro-Alvarez R, Lopez-Castroman J, Dorado P, Vaquero-Lorenzo C, Fernandez-Piqueras J *et al*. CYP2D6 poor metabolizer status might be associated with better response to risperidone treatment. *Pharmacogenet Genomics* 2013; **23**: 627–630.
- Remington G, Kapur S. Atypical antipsychotics: are some more atypical than others? *Psychopharmacology (Berl)* 2000; **148**: 3–15.
- Niculescu AB, Le-Niculescu H. Convergent Functional Genomics: what we have learned and can learn about genes, pathways, and mechanisms. *Neuropsychopharmacology* 2010; **35**: 355–356.
- Minguez P, Dopazo J. Functional genomics and networks: new approaches in the extraction of complex gene modules. *Expert Rev Proteomics* 2010; **7**: 55–63.
- Konradi C, Heckers S. Antipsychotic drugs and neuroplasticity: insights into the treatment and neurobiology of schizophrenia. *Biol Psychiatry* 2001; **50**: 729–742.
- Strand AD, Baquet ZC, Aragaki AK, Holmans P, Yang L, Cleren C *et al*. Expression profiling of Huntington's disease models suggests that brain-derived neurotrophic factor depletion plays a major role in striatal degeneration. *J Neurosci* 2007; **27**: 11758–11768.
- Korostynski M, Piechota M, Dzbek J, Mlynarski W, Szklarczyk K, Ziolkowska B *et al*. Novel drug-regulated transcriptional networks in brain reveal pharmacological properties of psychotropic drugs. *BMC Genomics* 2013; **14**: 606.
- Wei C, Li J, Bumgarner RE. Sample size for detecting differentially expressed genes in microarray experiments. *BMC Genomics* 2004; **5**: 87.
- Langfelder P, Horvath S. WGCNA: an R package for weighted correlation network analysis. *BMC Bioinformatics* 2008; **9**: 559.
- Minguez P, Götz S, Montaner D, Al-Shahrour F, Dopazo J. SNOW, a web-based tool for the statistical analysis of protein-protein interaction networks. *Nucleic Acids Res* 2009; **37**: W109–W114.
- Mas S, Gassó P, Parellada E, Bernardo M, Lafuente A. Network analysis of gene expression in peripheral blood identifies mTOR and NF-κB pathways involved in antipsychotic induced extrapyramidal symptoms. *Pharmacogenomics J*. epub ahead of print 27 Jan 2015.10.1038/tpj.2014.84.

- 21 Bindea G, Mlecnik B, Hackl H, Charoentong P, Tosolini M, Kirilovsky A et al. ClueGO: a Cytoscape plug-in to decipher functionally grouped gene ontology and pathway annotation networks. *Bioinformatics* 2009; **25**: 1091–1093.
- 22 Carretón O, Giral A, Torres-Peraza JF, Brito V, Lucas JJ, Ginés S et al. Age-dependent decline of motor neocortex but not hippocampal performance in heterozygous BDNF mice correlates with a decrease of cortical PSD-95 but an increase of hippocampal TrkB levels. *Exp Neurol* 2012; **237**: 335–345.
- 23 Giral A, Carretón O, Lao-Peregrin C, Martín ED, Alberch J. Conditional BDNF release under pathological conditions improves Huntington's disease pathology by delaying neuronal dysfunction. *Mol Neurodegener* 2011; **6**: 71.
- 24 Hales EC, Taub JW, Matherly LH. New insights into Notch1 regulation of the PI3K-AKT-mTOR1 signaling axis: targeted therapy of γ -secretase inhibitor resistant T-cell acute lymphoblastic leukemia. *Cell Signal* 2014; **26**: 149–161.
- 25 Laplante M, Sabatini DM. mTOR signaling at a glance. *J Cell Sci* 2009; **122**: 3589–3594.
- 26 Mas S, Gassó P, Malagelada C, Bernardo M, Lafuente A. Pharmacogenetic predictor of extrapyramidal symptoms induced by antipsychotics: multilocus interaction in the mTOR pathway. *Eur Neuropsychopharmacol* 2014; **25**: 51–59.
- 27 Schmidt RH, Jokinen JD, Massey VL, Falkner KC, Shi X, Yin X et al. Olanzapine activates hepatic mammalian target of rapamycin: new mechanistic insight into metabolic dysregulation with atypical antipsychotic drugs. *J Pharmacol Exp Ther* 2013; **347**: 126–135.
- 28 Shin SY, Lee KS, Choi YK, Lim HJ, Lee HG, Lim Y et al. The antipsychotic agent chlorpromazine induces autophagic cell death by inhibiting the Akt/mTOR pathway in human U-87MG glioma cells. *Carcinogenesis* 2013; **34**: 2080–2089.
- 29 Bonito-Oliva A, Pallottino S, Bertran-Gonzalez J, Girault JA, Valjent E, Fisone G. Haloperidol promotes mTORC1-dependent phosphorylation of ribosomal protein S6 via dopamine- and cAMP-regulated phosphoprotein of 32 kDa and inhibition of protein phosphatase-1. *Neuropharmacology* 2013; **72**: 197–203.
- 30 Costa-Mattioli M, Sossin WS, Klann E, Sonenberg N. Translational control of long-lasting synaptic plasticity and memory. *Neuron* 2009; **61**: 10–26.
- 31 Roux PP, Shahbazian D, Vu H, Holz MK, Cohen MS, Taunton J et al. RAS/ERK signaling promotes site-specific ribosomal protein S6 phosphorylation via RSK and stimulates cap-dependent translation. *J Biol Chem* 2007; **282**: 14056–14064.
- 32 Moore CE, Xie J, Gomez E, Herbert TP. Identification of cAMP-dependent kinase as a third in vivo ribosomal protein S6 kinase in pancreatic beta-cells. *J Mol Biol* 2009; **389**: 480–494.
- 33 Valjent E, Bertran-Gonzalez J, Bowling H, Lopez S, Santini E, Matamalas M et al. Haloperidol regulates the state of phosphorylation of ribosomal protein S6 via activation of PKA and phosphorylation of DARPP-32. *Neuropsychopharmacology* 2011; **36**: 2561–2570.
- 34 Bowling H, Zhang G, Bhattacharya A, Pérez-Cuesta LM, Deinhardt K, Hoeffler CA et al. Antipsychotics activate mTORC1-dependent translation to enhance neuronal morphological complexity. *Sci Signal* 2014; **7**: ra4.
- 35 Mannoury la Cour C, Salles MJ, Pasteau V, Millan MJ. Signaling pathways leading to phosphorylation of Akt and GSK-3 β by activation of cloned human and rat cerebral D₂ and D₃ receptors. *Mol Pharmacol* 2011; **79**: 91–105.
- 36 Beaulieu JM, Sotnikova TD, Marion S, Lefkowitz RJ, Gainetdinov RR, Caron MG. An Akt/beta-arrestin 2/PP2A signaling complex mediates dopaminergic neurotransmission and behavior. *Cell* 2005; **122**: 261–273.
- 37 Seo MS, Scarr E, Lai CY, Dean B. Potential molecular and cellular mechanism of psychotropic drugs. *Clin Psychopharmacol Neurosci* 2014; **12**: 94–110.
- 38 Dwivedi Y, Rizavi HS, Pandey GN. Differential effects of haloperidol and clozapine on [(3)H]cAMP binding, protein kinase A (PKA) activity, and mRNA and protein expression of selective regulatory and catalytic subunit isoforms of PKA in rat brain. *J Pharmacol Exp Ther* 2002; **301**: 197–209.
- 39 Mas S, Gassó P, Bernardo M, Lafuente A. Functional analysis of gene expression in risperidone treated cells provide new insights in molecular mechanism and new candidate genes for pharmacogenetic studies. *Eur Neuropsychopharmacol* 2013; **23**: 329–337.
- 40 Marder SR. Perspective: retreat from the radical. *Nature* 2014; **508**: S18.
- 41 Hyman SE. Perspective: revealing molecular secrets. *Nature* 2014; **508**: S20.

Supplementary Information accompanies the paper on the The Pharmacogenomics Journal website (<http://www.nature.com/tpj>)